ISBN: 978-3-95450-132-8 doi:10.18429/JACoW-IPAC2014-TUPRI014

MODELLING AND LONG TERM DYNAMICS OF CRAB CAVITIES IN THE LHC

R.B. Appleby*, D.R. Brett
School of Physics and Astronomy, The University of Manchester, UK
Cockcroft Institute, Daresbury Laboratory, Warrington, UK
J. Barranco García, EPFL, Lausanne, Switzerland and CERN, Geneva, Switzerland
R. De Maria, A. Grudiev, R. Tomás García, CERN, Geneva, Switzerland

Abstract

The High Luminosity upgrade of the Large Hadron Collider (HL-LHC) aims to achieve an integrated luminosity of 250-300 fb^{-1} per year. This upgrade includes the use of crab cavities to mitigate the geometric loss of luminosity arising from the beam crossing angle. The tight space constraints at the location of the cavities leads to cavity designs which are axially non-symmetric and have a potentially significant effect on the long term dynamics and dynamic aperture of the LHC. In this paper we present the current status of advanced modelling of crab cavities.

INTRODUCTION

The Large Hadron Collider (LHC) will be upgraded in the next decade, to increase the luminosity delivered to the experiments to 3000 fb^{-1} over 10 years, giving between 250-300 fb^{-1} per year. The target peak luminosity in this HL-LHC upgrade for the two high-luminosity experiments ATLAS and CMS is 20 10^{34}cm^{-2}s^{-1} (levelled during a fill to 5 10^{34}cm^{-2}s^{-1}) [1]. The primary technology upgrades forseen in this scenario include new high-field and large-aperture inner triplet quadrupoles based on the Nb_3Sn superconductor, use of crab cavities to recover head on collisions and perform luminosity leveling at interaction point 1 (IP1) and IP5, and various upgrade in the experiments to sustain higher luminosity levels. For more details see [1]. In order to fully benefit from upgraded optics, crab cavities are essential to counteract the geometric luminosity reduction due to a large crossing angle needed to overcome long range beam-beam interactions.

The crab cavities are RF deflecting cavities operated at a 90° phase shift, giving a z-dependent transverse kick to the particles in the bunch so that the bunch centre is undeflected and the head/tail receive a transverse kick. The total effect is a tilt of half the crossing angle ($\theta/2$) with respect to the uncrabbed motion at the IP. The crabbing arrangement in the LHC is to have a local crab bump closed about the IP. The crab cavities are to be located between the second separation dipole and the next matching quadrupole, which provides large β-functions and a phase advance to the IP of $\pi/2$ rad to minimize the required voltage. Furthermore, in order to close the crab orbit bump a second set of crab cavities after the IP at $\pi/2$ phase advance is needed.

* robert.appleby@manchester.ac.uk

There are currently many studies of crab cavity dynamics in the LHC, including long term stability studies [2, 3] and machine protection studies [4]. These calculations and simulations have required new techniques to accurately and efficiently model the dynamics in the crab cavities, often trading accuracy for computational speed and crab cavity models are crucial for understanding these new beam dynamaical effects. In this paper we present the current status of advanced modelling of crab cavities and consider the impact of the crab cavity on the LHC proton beam, involving multiple approaches and state of the art proton dynamics calculations. We present two models : the first is based on a multipole expansion of the integrated kick. This gives a quick and symplectic model. with the cavity described by a series of normal and skew multipoles. The second model is a potentially more accurate model using fitted vector potentials to model a thick crab cavity and expressing the transformation across the cavity in terms of a Taylor map derived from a symplectic integrator and a differential algebra approach. The cost is a very small symplectic error and increased speed of computation [5]. We shall present the two contrasting models and consider their relative merits.

THIN LENS RF MULTIPOLES

In this section we shall show that it is possible to model a crab cavity z-dependent kick with multipole coefficients extracted from EM simulations. The first approximation used is to represent the crab cavities by two drifts around a thin layer with lumped integrated kick. In this case it is assumed that the particle trajectory is not affected by the field while traversing the cavity and a kick is given to the particle at the centre of the cavity. Secondly, we assume that the trajectory is a straight line parallel to z (axial approximation). This implies that any B_s is neglected. Assuming these two approximations we can write for x (similar to y) thin lens kicks describing a change in transverse momentum derivable from the Hamiltonian,

$$H(x,y,z) = -\Re\left[\sum_{n=0}^{\infty} W_n(z)(x+iy)^n\right]\delta(s), \qquad (1)$$

where $W_n(z)$ is a z-dependent coefficient obtaineable from the integrated vector potential. This gives the longitudinal and transverse kicks as,

ISBN: 978-3-95450-132-8 doi:10.18429/JACoW-IPAC2014-TUPRI014

$$\Delta p_s = \Re\left[\sum_{n=0}^{\infty} W_n'(z)(x+iy)^n\right] \quad (2)$$

$$\Delta p_x + i\Delta p_y = \sum_{n=1}^{\infty} W_n(z)\frac{(x+iy)^{n-1}}{n}. \quad (3)$$

The strong non-axially symmetric shape of the compact cavities leads to a transverse dependency of the transverse kicks applied by the operating dipole mode. This effect can be described in a similar way as it is done in the analysis of static magnetic fields by means of an expansion of the transverse and longitudinal kicks, associated with the EM fields of the cavities, in terms of azimuthal multipoles [6, 7]. Assuming harmonic time dependence of complex EM fields and that the path through the cavity is rigid, the integrated vector potential can be reduced to the following form,

$$\int_0^L A_z ds = \sum_{n=1}^{N} \frac{1}{n}\rho^n (b_n \cos(n\phi) + a_n \sin(n\phi)) \quad (4)$$

where b_n and a_n are the normal and skew multipolar expansion coefficients of the complex EM fields, analogous to the description used for magnets but complex instead of real and N is the order of truncation of the azimuthal decomposition. This integrated vector potential is expressed in a thin-lens form, with no s dependence, and a_n and b_n are the integrated values over the length of the cavity. From the vector potential in this form the momentum change applied to a particle can be calculated in complex form and a momemtum kick applied to the beam.

The multipole coefficients are computed directly from meshed EM field data obtained from codes such as HFSS and a full set of coefficients can be found in [3]. There are mutiple ways to compute the normal and skew coefficents for the cavity, which we now describe.

Lorentz Force Starting from the general form of the Lorenz force law (LF) the transverse component of the force experienced by a particle moving along z-axis is given by,

$$F_\perp(\rho,\phi,s) = q\left[E_\perp + (\vec{v}\times\vec{B})_\perp\right]\exp\left(\mathrm{i}\frac{\omega s}{v}\right), \quad (5)$$

where ρ, ϕ and s are cylindrical coordinates, q is the particle charge and $\vec{E}$ and $\vec{B}$ are the complex electric and magnetic fields respectively. The momentum kick can be found from the force by integrating over the length of the cavity L, leading to explicit expressions for the multipole coefficients,

$$a_n = \frac{1}{qc}\frac{1}{\pi}\int_{-\pi}^{\pi}\frac{1}{\rho^{n-1}}\sin(n\phi)\int_0^L F_\rho(\rho,\phi,s)\,ds\,d\phi \quad (6)$$

$$b_n = \frac{1}{qc}\frac{1}{\pi}\int_{-\pi}^{\pi}\frac{1}{\rho^{n-1}}\cos(n\phi)\int_0^L F_\rho(\rho,\phi,s)\,ds\,d\phi. \quad (7)$$

This method requires knowledge of the electric and magnetic fields within the cavity.

Panofsky-Wenzel The Panofsky-Wenzel (PW) theorem [8] is a relationship between transverse and longitudinal kicks allowing the multipolar expansion coefficients calculation from the longitudinal electric field. Assuming the ultra relativistic case ($v \to c$) and no fringe fields beyond the edges of the integrable region $[0, L]$, the momentum change can be expressed in terms of E_z only, leading to expressions for the multipolar components in terms of a Fourier transformation of the electric field,

$$a_n = \frac{in}{\omega}\frac{1}{\pi}\int_{-\pi}^{\pi}\frac{1}{\rho^n}\sin(n\phi)\int_0^L e^{\mathrm{i}\frac{\omega}{c}s}E_z(\rho,\phi,s)\,ds\,d\phi \quad (8)$$

$$b_n = \frac{in}{\omega}\frac{1}{\pi}\int_{-\pi}^{\pi}\frac{1}{\rho^n}\cos(n\phi)\int_0^L e^{\mathrm{i}\frac{\omega}{c}s}E_z(\rho,\phi,s)\,ds\,d\phi. \quad (9)$$

The multipoles obtained from this method agree with those obtained from the LF method [3].

TAYLOR MAP CAVITY MODELS

Producing an analytical representation of the field allows for a Hamiltonian-based analysis of the particle dynamics of the operating mode. The field fitting method [9] assumes the vacuum form of Maxwell's equations is valid for a finite volume through the length of the cavity and that the field obeys the Helmholtz equation.

The longitudinal field may be expressed as an infinite series of cylindrical harmonic modes, where a boundary is chosen such that the harmonic functions describe the field within a cylinder running the length of the cavity. The field fitting method [9] expresses the field (and the associated vector potential) analytically, given explicit field data on the surface of the cylinder. Further details can be found in [2, 9]. The electric field $\vec{E}$ contained within the vacuum of an RF cavity satisfies the wave equation,

$$\nabla^2\vec{E} - \frac{1}{c^2}\frac{\partial^2\vec{E}}{\partial t^2} = 0. \quad (10)$$

It is assumed that for a standing wave mode in a cavity, the $\vec{E}$ field has a harmonic time dependence, and the spatial and time dependent field components are separable, so that the spatial part obeys the vector Helmholtz equation

$$\nabla^2\vec{E}^{(l)} + k_l^2\vec{E}^{(l)} = 0, \quad (11)$$

where $k_l \equiv \omega_l/c$. The electric and magnetic fields, and hence the vector potential, can be expressed completely in terms of a set of functions ($\tilde{e}_n(k)$, $\tilde{f}_n(k)$, $\tilde{\beta}_n(k)$ and $\tilde{\alpha}_n(k)$, where k is a Fourier variable and n a mode number). These functions are obtainable from knowledge of the field on the surface of a cylinder inscribed inside the cavity volume and give access to the electric and magnetic fields for $\rho < R$.

Figure 1 gives an example of the achievable fit, showing the relative fitting error of the longitudinal electric field in the 4-rod crab cavity [10]. The solid line is an interpolation of the field data, the squares show the fitted electric field using the methods described in this section and the crosses show a Taylor expansion of the fitted fields equations [2] suitable for further beam dynamics studies.

ISBN: 978-3-95450-132-8 doi:10.18429/JACoW-IPAC2014-TUPRI014

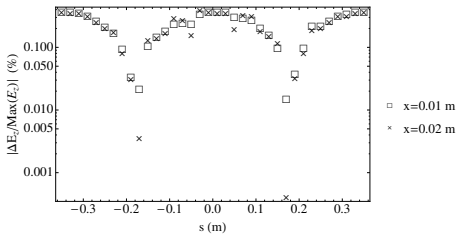

Figure 1: The residual error of the fitted 4-rod crab cavity longitudinal electric field.

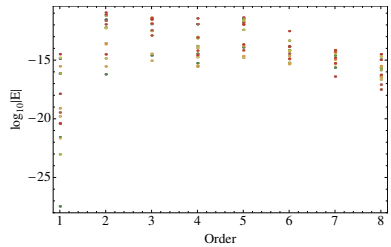

Figure 2: The symplectic error of the crab cavity Taylor map as a function of series order.

The crab cavity Taylor maps are produced using an explicit symplectic integrator developed by Wu, Forest, and Robin [11] (WFR) implemented in a diffential algebra code. The WFR integrator was developed for an s dependent Hamiltonian for charged particles moving through an electromagnetic field. The Hamiltonian takes the following form,

$$H = -\sqrt{\left(\frac{1}{\beta_0}+\delta\right)^2 - (p_x - a_x)^2 - (p_y - a_y)^2 - \frac{1}{\gamma_0^2\beta_0^2}} - a_s + \frac{\delta}{\beta_0} + p_s \quad (12)$$

where $a_{x,y,s}(x,y,z,s)$ are the normalised vector potentials, x, p_x, y, p_y are the canonical variables describing transverse positions and conjugate momenta, z and δ are the relative position to the synchronous particle and relative energy. γ_0 and β_0 are the reference relativistic factors corresponding to the reference momentum. The Hamiltonian is extended to four conjugate pairs, with the fourth $\{s, p_s\}$ allowing motion along the reference trajectory through an s dependent vector field [11]. A Taylor map expresses the relationship between the initial and final state variables in the form of a Taylor series,

$$x_k^f = f_k(x_1^i, \ldots, x_6^i), \quad (13)$$

where,

$$f_k(x_1^i, \ldots, x_6^i) = \sum_{i_1,\ldots,i_6=0}^{\sum_j^6 i_j = \text{Order}} A_{k,i_1,\ldots,i_6} \prod_{j=1}^{6} (x_j^i)^{i_j}, \quad (14)$$

where the order of a Taylor map is determined by the largest total power of any term in the series. x_j^i are the initial values of the canonical variables, i_j are the exponents, and $A_{k,i_1\ldots i_6}$ is the coefficient of term defined by the exponents in the series f_k. To calculate a Taylor map the numerical integration must be carried out using a differential algebra library, which considers all variables as a truncated power series. The WFR integrator [11] is then used to integrate through the analytic vector potential.

Truncating the Taylor map introduces a symplectic error, which leads to a failure to conserve the phase space volume during long term simulations of particle motion. The amount of error is expressed through the coefficients of the E matrix,

$$E(\vec{x}^i) = J^T(\vec{x}^i) \cdot S \cdot J(\vec{x}^i) - S. \quad (15)$$

where J is the Jacobian of the map and S is the standard symplectic matrix. For a Taylor map (step size of 0.01 m) trucated at order eight, the symplectic error up to eighth order is shown in Fig. 2, evaluated at a single point in phase space. The first order map has least symplectic error as its only source of error comes from the machine precision (double precision) rather than the series truncation, hence the symplectic error is at the level of 10^{-15}. Note the a_n and b_n coefficients of the multipole method can be obtained from field fitting, and show agreement, as discussed in [3].

MERITS OF THE APPOACHES AND CONCLUSION

We have described the approaches taken to model crab cavities for the LHC upgrade in recent work. The first is built around a single thin lens cavity kick obtained from two different ways from integrals over the cavity field. The resulting cavity multipoles assume ultra-relativistic rigid beams and a beam parallel to the axis. The full set of cavity multipoles obtained from all methods and for all cavities can be found in [3]. This approach ensures a fully symplectic cavity model and has the virtue of low computational cost.

The second method using the field fitting methods of [9] to construct an analytic vector potential for the crab cavity directly from EM field data. A symplectic integrator and a differential algebra code is used to represent the transformation of the crab cavity as a Taylor map, giving accurate dynamics [5] but at the cost of a symplectic error on the level of machine precision due to the truncation of the Taylor series. Detailed studies comparing the two methods have been performed in [2].

In conclusion, there has been a lot of work on the modelling and dynamics of crab cavities in the LHC. This paper describes the different cavity modelling approaches used in this work and contrasts the two. The use of these models for long term stability in the LHC is described in [2].

ACKNOWLEDGMENT

The HiLumi LHC Design Study is included in the High Luminosity LHC project and is partly funded by the European Commission within the Framework Programme 7 Capacities Specific Programme, Grant Agreement 284404.

REFERENCES

[1] Rossi L., "LHC Upgrade Plans: Options and Strategy", (2011).

ISBN: 978-3-95450-132-8 doi:10.18429/JACoW-IPAC2014-TUPRI014

[2] D. R. Brett et al., "Realistic crab cavity modelling for the high luminosity large hadron collider," submitted to Phys. Rev. ST Accel. Beams.

[3] J. Barranco García et al., "Long term dynamics of the Large Hadron Collider with crab cavity multipoles," submitted to Phys. Rev. ST Accel. Beams.

[4] B. Yee-Rendon, Phys. Rev. ST Accel. Beams 17, 051001 (2014).

[5] D.R. Brett, R.B. Appleby, G. Burt, and B. Hall, "Particle trajectories in a four rod crab cavity," Nuclear Instruments and Methods in Physics Research Section A: Accelerators, Spectrometers, Detectors and Associated Equipment 734, Part A, 79 – 83 (2014).

[6] J. Barranco Garcia, R. Calaga, R. De Maria, et al., in Proceedings of the 2012 International Particle Accelerator Conference, New Orleans, USA (2012).

[7] Goldberg, D.A.; Lambertson, G.R., "Dynamic devices: A primer on pickups and kickers", 1991.

[8] W Panofsky and W Wenzel, "Some considerations concerning the transverse deflection of charged particles in radiofrequency fields," Review of Scientific Instruments 27, 967 (1956).

[9] Dan Abell, "Numerical computation of high-order transfer maps for rf cavities," Phys. Rev. ST Accel. Beams 9, 052001 (2006).

[10] G. Burt et al., "4 Rod RF Design," (Presented at 5th LHC CC workshop, Geneva, Switzerland, 2011).

[11] Y.K Wu et al, Phys. Rev. E 68, 046502 (2003).